transformation capabilities is invaluable in the design of balanced microwave circuits such as mixers, push–pull amplifiers, and frequency doublers.

ACKNOWLEDGMENT

The authors would like to thank M. Blewett and D. Granger for their technical support in fabricating the circuits.

REFERENCES

[1] T. Chen *et al.*, "Broadband monolithic passive baluns and monolithic double balanced mixer," *IEEE Trans. Microwave Theory Tech.*, vol. 39, pp. 1980–1986, Dec. 1991.
[2] P. C. Hsu, C. Nguyen, and M. Kintis, "Uniplanar broad-band push–pull FET amplifiers," *IEEE Trans. Microwave Theory Tech.*, vol. 45, pp. 2150–2152, Dec. 1997.
[3] S. A. Maas and Y. Ryu, "A broadband, planar, monolithic resistive frequency doubler," in *IEEE Int. Microwave Symp. Dig.*, 1994, pp. 443–446.
[4] A. M. Pavio and A. Kikel, "A monolithic or hybrid broadband compensated balun," in *IEEE Int. Microwave Symp. Dig.*, 1990, pp. 483–486.
[5] W. R. Brinlee, A. M. Pavio, and K. R. Varian, "A novel planar double-balanced 6–18 GHz MMIC mixer," in *IEEE Microwave Millimeter-Wave Monolithic Circuit Symp. Dig.*, 1994, pp. 139–142.
[6] M. C. Tsai, "A new compact wide-band balun," in *IEEE Microwave and Millimeter Wave Monolithic Circuit Symp. Dig.*, 1993, pp. 123–125.
[7] K. Nishikawa, I. Toyoda, and T. Tokumitsu, "Compact and broad-band three-dimensional MMIC balun," *IEEE Trans. Microwave Theory Tech.*, vol. 47, pp. 96–98, Jan. 1999.
[8] Y. J. Yoon *et al.*, "Design and characterization of multilayer spiral transmission-line baluns," *IEEE Trans. Microwave Theory Tech.*, vol. 47, pp. 1841–1847, Sept. 1999.
[9] N. Marchand, "Transmission line conversion transformers," *Electronics*, vol. 17, no. 12, pp. 142–145, Dec. 1944.
[10] C. M. Tsai and K. C. Gupta, "A generalized model for coupled lines and its applications to two-layer planar circuits," *IEEE Trans. Microwave Theory Tech.*, vol. 40, pp. 2190–2099, Dec. 1992.
[11] R. Schwindt and C. Nguyen, "Computer-aided analysis and design of a planar multilayer Marchand balun," *IEEE Trans. Microwave Theory Tech.*, vol. 42, pp. 1429–1434, July 1994.
[12] R. H. Jansen, J. Jotzo, and R. Engels, "Improved compactions of a planar multilayer MMIC/MCM baluns using lumped element compensation," in *IEEE Int. Microwave Symp. Dig.*, 1997, pp. 227–280.
[13] T. Wang and K. Wu, "Size-reduction and band-broadening design technique of uniplanar hybrid coupler technique of uniplanar hybrid ring coupler using phase inverter for M(H)MIC's," *IEEE Trans. Microwave Theory Tech.*, vol. 47, pp. 198–206, Feb. 1999.
[14] S. A. Maas, *Microwave Mixers*, 2nd ed. Norwood, MA: Artech House, 1992.

A Novel Interpretation of Transistor S-Parameters by Poles and Zeros for RF IC Circuit Design

Shey-Shi Lu, Chin-Chun Meng, To-Wei Chen, and Hsiao-Chin Chen

***Abstract*—In this paper, we have developed an interpretation of transistor S-parameters by poles and zeros. The results from our proposed method agreed well with experimental data from GaAs FETs and Si MOSFET's. The concept of source-series feedback was employed to analyze a transistor circuit set up for the measurement of the S-parameters. Our method can describe the frequency responses of all transistor S-parameters very easily and the calculated S-parameters are scalable with device sizes. It was also found that the long-puzzled kink phenomenon of S_{22} observed in a Smith chart can be explained by the poles and zeros of S_{22}.**

***Index Terms*—Poles, S-parameters, transistors, zeros.**

I. INTRODUCTION

Wireless circuit design has recently become an important field all over the world. However, as far as RF circuit design is concerned, microwave circuit designers are talking about S-parameters, while analog circuit designers are thinking in terms of poles and zeros. Obviously, there is a gap between the thought processes of microwave circuit engineers and analog circuit engineers. For a long time, S-parameters have been understood in terms of Y- or Z-parameters. These Y- or Z-parameters, though very useful in calculating S-parameters, cannot give insight into the behaviors or physical meanings of S-parameters. For example, it is difficult for Y- or Z-parameters to describe the frequency responses of S-parameters directly or to explain the kink behavior of S_{22} observed in a Smith chart [1], such as the one shown in Fig. 1. In this paper, we present an interpretation of S-parameters from a poles' and zeros' point-of-view. By doing this, we can predict the frequency responses of S-parameters very easily and explain the kink behavior of S_{22} in Smith charts. Our calculated values of transistor S-parameters showed excellent agreement with the experimental data from 0.25-μm-gate Si MOSFETs and sub-micrometer gate GaAs FETs with different gate width.

II. THEORY

First, consider the circuit shown in Fig. 2(a), where an FET is connected for the measurement of its S-parameters. S_{11} and S_{21} can be measured by setting $V_2 = 0$ and $V_1 \neq 0$, while S_{22} and S_{12} can be measured by setting $V_1 = 0$ and $V_2 \neq 0$. Z_{O1} at input port and Z_{O2} at output port are both equal to 50 Ω, but are intentionally labeled differently. The reason for this will become clear later on. In general, the circuit in Fig. 2(a) is not easy to handle. However, the problem will be much easier to solve if this circuit is viewed as a dual feedback circuit, in which R_s is the local series–series feedback element and $C_{\rm gd}$ the local shunt–shunt feedback element. In order to simplify circuit analysis, we temporarily neglect the inductors and transform the circuit of Fig. 2(a) into that of Fig. 2(b) by using local series–series feedback

Manuscript received December 9, 1999. This work was supported under Grant 89-E-FA06-2-4, under Grant NSC89-2219-E-002-044, and under Grant NSC88-2219-E-005-003.

S.-S. Lu, T.-W. Chen, and H.-C. Chen are with the Department of Electrical Engineering, National Taiwan University, Taipei, Taiwan 10617, R.O.C. (e-mail: sslu@cc.ee.ntu.edu.tw).

C.-C. Meng is with the Department of Electrical Engineering, Chung-Hsing University, Taichung, Taiwan 40227, R.O.C.

Publisher Item Identifier S 0018-9480(01)01089-4.

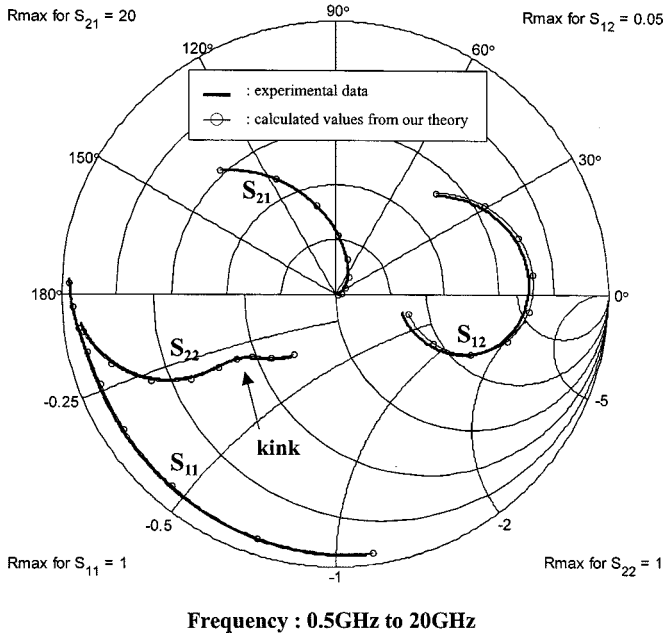

Fig. 1. Comparison of the experimental and calculated S-parameters of a sub-micrometer gate GaAs FET with gate width of 4 mm on a Smith chart. —: experimental data. -⊖-: calculated values by our theory. Note that the kink phenomenon of S_{22} is indicated by an arrow.

theory [2] with some necessary circuit element modifications as follows:

$$C'_{\rm gs} = \frac{C_{\rm gs}}{1 + g_m R_S} \tag{1}$$

$$R'_i = R_i + R_S \tag{2}$$

$$C'_{\rm ds} = \frac{C_{\rm ds}}{1 + g_m R_S} \tag{3}$$

$$R'_{\rm ds} = R_{\rm ds} \cdot (1 + g_m R_S) \tag{4}$$

$$C'_{\rm gd} = C_{\rm gd} \tag{5}$$

$$g'_m = \frac{g_m}{1 + g_m \cdot R_S} \tag{6}$$

where $g_m = g_{mo} \cdot \exp(-j\omega\tau)$ and g_{mo} is the dc transconductance and all the other symbols have their usual meanings.

Set $V_2 = 0$ and $V_1 \neq 0$ for the discussions of S_{11} and S_{21}. If the input impedance seen to the right-hand side of Z_{O1} in Fig. 2(b) is denoted by $Z_{\rm in}$, then S_{11} is given by

$$S_{11} = \frac{Z_{\rm in} - Z_{O1}}{Z_{\rm in} + Z_{O1}}. \tag{7}$$

By definition, the poles of S_{11} are the roots of $L(s) = Z_{\rm in} + Z_{O1} = 0$. $Z_{\rm in}$ can be calculated and $L(s) = 0$ can be proven to be equivalent to equation $D(s) = 0$ given by

$$\begin{aligned} D(s) = 1 &+ s\left[C'_{\rm gs}\left(Z_{O1} + R_g + R'_i\right) + C'_{\rm ds}(Z_{O2} + R_d)\right. \\ &+ C'_{\rm gd}\left(g'_m(Z_{O1} + R_g)(Z_{O2} + R_d)\right. \\ &\left.\left.+ (Z_{O1} + R_g) + (Z_{O2} + R_d)\right)\right] + s^2 \\ &\cdot \left[\left(C'_{\rm gd}C'_{\rm gs} + C'_{\rm gd}C'_{\rm ds} + C'_{\rm gs}C'_{\rm ds}\right)(Z_{O1} + R_g)\right. \\ &\cdot (Z_{O2} + R_d) + \left(C'_{\rm gs}C'_{\rm gd} + C'_{\rm gs}C'_{\rm ds}\right)R'_i \\ &\left.\cdot (Z_{O2} + R_d) + C'_{\rm gs}C'_{\rm gd}R'_i(Z_{O1} + R_g)\right] \\ &+ s^3 C'_{\rm gs}C'_{\rm gd}C'_{\rm ds}R'_i(Z_{O1} + R_g)(Z_{O2} + R_d) = 0. \end{aligned} \tag{8}$$

The expression of $D(s)$ in (8) may be complicated at a first glance because it involves a cubic equation. However, usually R'_i can be neglected, as well as the product of $R'_i C'_{\rm ds}$. Thus, (8) is reduced to a

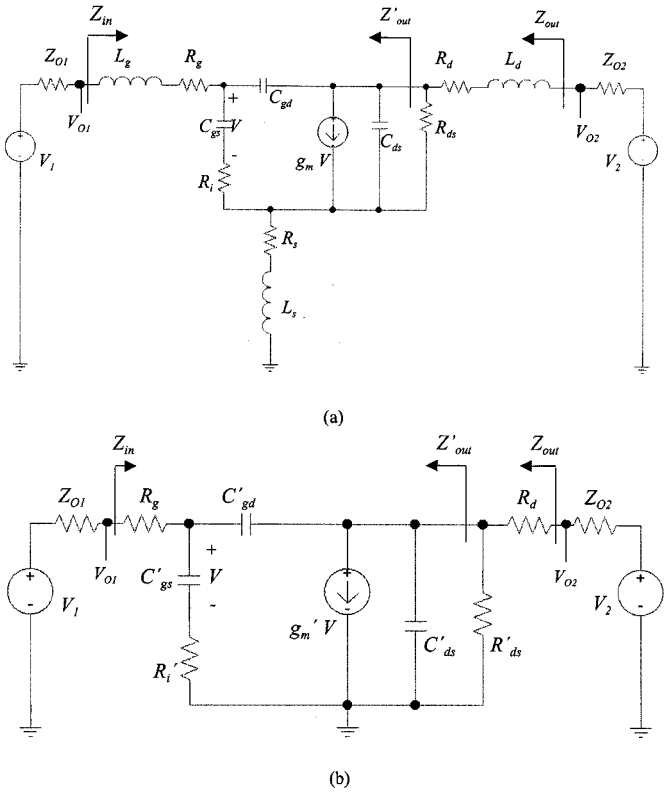

Fig. 2. Setup for the measurement of transistor S-parameters. (a) Complete circuit. (b) Simplified circuit with the local series–series feedback element (R_S) absorbed.

quadratic equation as follows, by which two poles ω_{p1} and ω_{p2} can be solved easily:

$$\begin{aligned} D(s) = 1 &+ s\left[C'_{\rm gs}(Z_{O1} + R_g) + C'_{\rm ds}(Z_{O2} + R_d)\right. \\ &+ C'_{\rm gd}(g'_m(Z_{O1} + R_g)(Z_{O2} + R_d) \\ &\left.+ (Z_{O1} + R_g) + (Z_{O2} + R_d))\right] \\ &+ s^2\left[\left(C'_{\rm gd}C'_{\rm gs} + C'_{\rm gd}C'_{\rm ds} + C'_{\rm gs}C'_{\rm ds}\right)\right. \\ &\left.\cdot (Z_{O1} + R_g)(Z_{O2} + R_d)\right] = 0. \end{aligned} \tag{9}$$

For the discussions that follows, for convenience, we will call (8) the three-pole approximation and (9) the two-pole approximation. In solving (9), the method of dominant pole approximation [3] can be utilized if a dominant pole indeed exists, i.e., the lowest frequency pole is at least two octaves lower than the other pole. As an illustrative example, the solutions (poles) of (9) found by the dominant pole approximation are listed in Table I.

The zeros of S_{11} are the roots of $Z(s) = Z_{\rm in} - Z_{O1} = 0$. This zero equation can be viewed as the transformation of the pole equation $L(s) = Z_{\rm in} + Z_{O1} = 0$ with Z_{O1} in $L(s)$ is replaced by $-Z_{O1}$. Equivalently, the zero equation of S_{11}, which we call $N1(s) = 0$, can be obtained easily by replacing Z_{O1} in $D(s) = 0$ with $-Z_{O1}$. At dc frequency, $S_{11} = 1$ because $C'_{\rm gs}$ and $C'_{\rm gd}$ are open circuits and, therefore, S_{11} can be written as follows for all frequencies:

$$\begin{aligned} S_{11} &= \frac{Z_{\rm in} - Z_{O1}}{Z_{\rm in} + Z_{O1}} \\ &= 1 \cdot \frac{N1(s)}{D(s)} \\ &\cong 1 \cdot \frac{\left(1 + \dfrac{s}{\omega_{Z1}}\right)\left(1 + \dfrac{s}{\omega_{Z2}}\right)}{\left(1 + \dfrac{s}{\omega_{P1}}\right)\left(1 + \dfrac{s}{\omega_{P2}}\right)} \end{aligned} \tag{10}$$

where ω_{Z1} and ω_{Z2} are the two zeros of S_{11}.

The physical meaning of S_{21} is twice that of the voltage gain V_{O2}/V_1. Since the poles of all the four S-parameters are the same, S_{21} can be given easily by the inspection of Fig. 2(b) as follows:

$$S_{21} = \frac{V_{O2}}{V_1} \cdot 2 \left(1 - \frac{sC'_{\rm gd}}{\dfrac{g'_m}{1 + sC'_{\rm gs}R'_i}} \right) = -2A_M \frac{}{D(s)} \cong -2A_M \frac{\left(1 - \dfrac{s}{\omega_{Z5}}\right)}{\left(1 + \dfrac{s}{\omega_{P1}}\right)\left(1 + \dfrac{s}{\omega_{P2}}\right)} \tag{11}$$

where $A_M = g'_m Z_{O2}(R'_{\rm ds} \| (R_d + Z_{O2}))/(Z_{O2} + R_d)$ is the midband gain of $V_O 2/V_1 \cdot \omega_{Z5} = g'_m/C'_{\rm gd}$.

We now turn our attention into S_{22} and S_{12} by setting $V_1 = 0$ and $V_2 \neq 0$. If the output impedance seen to the left-hand side of Z_{O2} is denoted by $Z_{\rm out}$, then S_{22} is given by

$$S_{22} = \frac{Z_{\rm out} - Z_{O2}}{Z_{\rm out} + Z_{O2}} = \frac{R'_{\rm ds} + R_d - Z_{O2}}{R'_{\rm ds} + R_d + Z_{O2}} \cdot \frac{N2(s)}{D(s)} \cong \frac{R'_{\rm ds} + R_d - Z_{O2}}{R'_{\rm ds} + R_d + Z_{O2}} \cdot \frac{\left(1 + \dfrac{s}{\omega_{Z3}}\right)\left(1 + \dfrac{s}{\omega_{Z4}}\right)}{\left(1 + \dfrac{s}{\omega_{P1}}\right)\left(1 + \dfrac{s}{\omega_{P2}}\right)} \tag{12}$$

where $N2(s)$ is the zero equation of S_{22} and is obtained by replacing Z_{O2} in $D(s) = 0$ with $-Z_{O2}$. ω_{Z3} and ω_{Z4} are the zeros of S_{22}. The factor $(R'_{\rm ds} + R_d - Z_{O2})/(R'_{\rm ds} + R_d + Z_{O2})$ is the reflection coefficient that V_2 "sees" at dc frequency.

As for S_{12}, the physical meaning of S_{12} is twice that of the voltage gain V_{O1}/V_2. S_{12} is given by the inspection of Fig. 2(b) as follows:

$$S_{12} = 2 \cdot \frac{R'_{\rm ds}}{R'_{\rm ds} + R_d + Z_{O2}} \cdot sC'_{\rm gd} Z_{O1} \frac{1}{D(s)} \cong 2 \cdot \frac{R'_{\rm ds}}{R'_{\rm ds} + R_d + Z_{O2}} \cdot \frac{sC'_{\rm gd} Z_{O1}}{\left(1 + \dfrac{s}{\omega_{P1}}\right)\left(1 + \dfrac{s}{\omega_{P2}}\right)} \tag{13}$$

where $(R'_{\rm ds} \cdot sC'_{\rm gd} \cdot Z_{O1})/(R'_{\rm ds} + R_d + Z_{O2})$ is the gain of V_{O1}/V_2 at low frequencies.

III. Experimental Results and Discussions

(1)–(13) have been applied to Fujitsu GaAs FETs with different gate width (0.5, 1, 2, and 4 mm). The effects of inductors in the circuit of Fig. 2(a) were included by replacing R_g, R_s, and R_d with $R_g + j\omega L_g$, $R_s + j\omega L_s$, and $R_d + j\omega L_d$ in related formulas, respectively. The S-parameters of the transistor with gate width of 4 mm were plotted in a Smith chart, as shown in Fig. 1. Excellent agreement between calculated values and experimental data [4] can be seen clearly in Fig. 1. The method has been applied to Si MOSFETs with good agreement as well.

The frequency responses of the four S-parameters of the Fujitsu GaAs FETs with gate width of 2 mm are shown in Fig. 3(a) and (b), respectively. The characteristics of the devices with gate width of 0.5 and 1 mm are similar to those of the device with gate width of 2 mm and, therefore, for clarity, are not shown in Fig. 3(a) and (b). The S-parameters of the device with gate width of 4 mm also shows similar frequency responses, except for its S_{22}, whose frequency response is, therefore, included in Fig. 3(b), as well as for comparison. The locations of poles and zeros have to be known in order to discuss the characteristics of the frequency responses of these S-parameters. In general, it involves solving the cubic equation of (8) to find the three poles, which is, of course, difficult. However, as we mentioned previously, if the third-order term is negligible, then (8) becomes quadratic equation (9), which can be solved easily. As can be seen clearly in Fig. 3(a) and (b), the two-pole approximation based on (9) indeed gives very satisfactory results. Dominant pole (zero) approximation can be used to obtain the expressions of the poles and zeros. The results are given in Table I. It can be shown that the expression of the second pole ω_{p2} given in Table I has the physical meaning of the inverse of the time constant of the parallel combination of $Z'_{\rm out}$, $R'_{\rm ds}$, and $R_d + Z_{O2}$. A significant advantage of our theory is that, once the expressions of the two poles are known, the expressions of the zeros of S_{11} and S_{22} are readily obtained. The zeros of S_{11}, ω_{Z1}, and ω_{Z2} can be obtained easily by replacing Z_{O1} with $-Z_{O1}$ in the expressions of ω_{p1} and ω_{p2}, respectively. The zeros of S_{22}, ω_{Z3}, and ω_{Z4} can be obtained easily by replacing Z_{O2} with $-Z_{O2}$ in the expressions of ω_{p1} and ω_{p2}, respectively.

From (11) and the two-pole approximation, the frequency response of S_{21} has two poles and one zero. This zero is usually much larger than the two poles, which results in the shape of the Bode plot of $|S_{21}|$

TABLE I
Expressions of Poles and Zeros of S_{11} and S_{22} by Dominant Pole (Zero) Approximation

Poles of S-parameters	$\omega_{p1} = \left(C'_{gs}Z_{01P}+C'_{gd}(1+g'_mZ_{02P})Z_{01P}+(C'_{gd}+C'_{ds})Z_{02P}\right)^{-1}$ $\omega_{p2} = \dfrac{\left[(Y_{01P}+g'_m)\dfrac{C'_{gd}}{C'_{gs}+C'_{gd}} + Y_{01P}\dfrac{C'_{ds}}{C'_{gs}+C'_{gd}} + Y_{O2P}\right]}{\dfrac{C'_{gs}C'_{gd}}{C'_{gs}+C'_{gd}} + C'_{ds}}$
Zeros of S_{11}	$\omega_{z1} = \left(C'_{gs}Z_{01Z}+C'_{gd}(1+g'_mZ_{02P})Z_{01Z}+(C'_{gd}+C'_{ds})Z_{02P}\right)^{-1}$ $\omega_{z2} = \dfrac{\left[(Y_{01Z}+g'_m)\dfrac{C'_{gd}}{C'_{gs}+C'_{gd}} + Y_{01Z}\dfrac{C'_{ds}}{C'_{gs}+C'_{gd}} + Y_{O2P}\right]}{\dfrac{C'_{gs}C'_{gd}}{C'_{gs}+C'_{gd}} + C'_{ds}}$
Zeros of S_{22}	$\omega_{z3} = \left(C'_{gs}Z_{01P}+C'_{gd}(1+g'_mZ_{02Z})Z_{01P}+(C'_{gd}+C'_{ds})Z_{02Z}\right)^{-1}$ $\omega_{z4} = \dfrac{\left[(Y_{01P}+g'_m)\dfrac{C'_{gd}}{C'_{gs}+C'_{gd}} + Y_{01P}\dfrac{C'_{ds}}{C'_{gs}+C'_{gd}} + Y_{O2Z}\right]}{\dfrac{C'_{gs}C'_{gd}}{C'_{gs}+C'_{gd}} + C'_{ds}}$
definition of some symbols	$Z_{01P} \equiv R_d + Z_{O1}$ $\quad Y_{01P} \equiv 1/Z_{01P}$ $Z_{02P} \equiv (R_g + Z_{O2}) \| R'_{ds}$ $\quad Y_{02P} \equiv 1/Z_{02P}$ $Z_{01Z} \equiv R_d - Z_{O1}$ $\quad Y_{01Z} \equiv 1/Z_{01Z}$ $Z_{02Z} \equiv (R_g - Z_{O2}) \| R'_{ds}$ $\quad Y_{02Z} \equiv 1/Z_{02Z}$

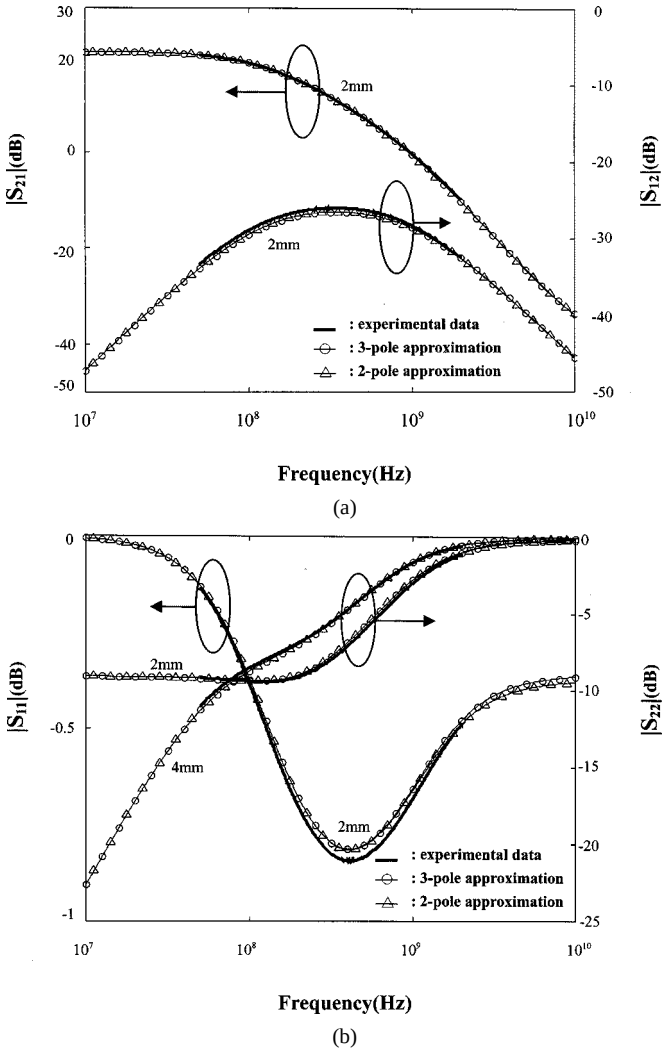

Fig. 3. Frequency responses of the magnitude of the four S-parameters of a Fujitsu sub-micrometer gate GaAs FET with gate width of 2 mm. (a) S_{21} and S_{12}. (b) S_{11} and S_{22}. —: experimental data. -⊖-: three-pole approximation. -△-: two-pole approximation. The frequency responses of the other size FETs show similar characteristics, except for the one with 4-mm gate width, whose S_{22} behaves differently.

shown in Fig. 3(a). From Fig. 3(a), the first pole ω_{p1} has the physical meaning of 3-dB bandwidth of the voltage gain S_{21}.

From (10) and the two-pole approximation, S_{11} has two poles and two zeros. The shape of the frequency response of $|S_{11}|$ is dependent on the locations of its two zeros with respect to its two poles. From Table I, it is easy to see that the two zeros fall between the two poles and, therefore, a dip will occur in a Bode plot of $|S_{11}|$, as can be seen in Fig. 3(b).

According to (12) and the two-pole approximation, S_{22} has two poles and two zeros just like the case of S_{11}. The two zeros of S_{22} fall between its two poles in the cases of 0.5, 1, and 2 mm. Hence, a dip is observed in the Bode plot of $|S_{22}|$, as shown in Fig. 3(b), which is one reason that causes the kink phenomenon of S_{22} observed in a Smith chart. The kink effect in S_{22} for a smaller device (0.5 mm) or in S_{11} for all sizes of devices are obscured by pole–zero cancellation. When the device size is increased to 4 mm, ω_{Z3} of S_{22} becomes smaller than ω_{P1} and, thus, $|S_{22}|$ looks like a sloped step, as shown in Fig. 3(b). The alternative appearance of poles and zeros is another reason for the kink phenomenon of S_{22} observed in a Smith chart (see Fig. 1).

According to (13) and the two-pole approximation, S_{12} has two poles and one zero. This zero occurs at zero frequency and explains the bell-shape frequency response of $|S_{12}|$ in Fig. 3(a) well.

IV. Conclusions

In summary, the S-parameters of transistors have been interpreted in terms of poles and zeros. All the four S-parameters have the same two poles. It is found that the two zeros of S_{11} always fall between its two poles and, hence, a dip is observed in the frequency response of $|S_{11}|$. The locations of the two zeros of S_{22} with respect to its two poles are dependent on the device size. For smaller transistors, S_{22} behaves similarly to S_{11}. For larger transistors, one zero of S_{22} becomes smaller than its first pole and, therefore, the shape of a sloped step is observed, which is one reason for the kink phenomenon of S_{22} observed in a Smith chart. S_{12} has a zero at zero frequency and this explains why the frequency response of $|S_{12}|$ looks like a bell shape. Our proposed method thus provides a certain insight into the behavior of the S-parameters and, hence, may be helpful for RF integrated circuit (RFIC) designs.

References

[1] B. Bayrajtariglu, N. Camilleri, and S. A. Lambert, "Microwave performance of n-p-n and p-n-p AlGaAs/GaAs heterojunction bipolar transistors," *IEEE Trans. Microwave Theory Tech.*, vol. 36, pp. 1869–1873, Dec. 1988.

[2] P. R. Gray and R. G. Meyer, *Analysis and Design of Analog Integrated Circuits*. New York: Wiley, 1993, pp. 579–584.

[3] A. S. Sedra and K. C. Smith, *Microelectronic Circuits*, 4th ed. Oxford, U.K.: Oxford Univ. Press, 1993, pp. 595–601.

[4] Y. Aoki and Y. Hirano, "High-power GaAs FETs," in *High Power GaAs FET Amplifiers*, J. L. B. Walker, Ed. Norwood, MA: Artech House, 1993, p. 81.